

Diffraction and the Evolution of Small-Scale Filaments in a Laser-Produced Plasma

R. Rankin, C. E. Capjack, and C. R. James

Department of Electrical Engineering, The University of Alberta, Edmonton, Canada T6G 2G7

(Received 16 March 1988)

Intense laser light filamentation in a hydrogen plasma is investigated using a two-dimensional hydrodynamic simulation code. The laser paraxial wave equation is used to study the focusing which results from a Gaussian hot-spot intensity perturbation. It is found that diffraction increases the scale size of small-scale off-axis filamentation, and significantly raises the ponderomotive self-focusing intensity threshold. Radially propagating density fluctuations, contributing to small-scale focusing, are observed due to the self-consistent treatment of hydrodynamics in the simulations.

PACS numbers: 52.40.Nk, 52.50.Jm, 52.65.+z

The interest in short wavelength ($\lambda \approx 0.25 \mu\text{m}$) lasers, for direct drive inertial confinement fusion, results from predictions that anomalous scattering and absorption processes will become significantly less important. However, self-focusing of the laser light may cause a number of unwanted effects to reappear. In particular, the high intensity of the filamented light can drive parametric instabilities, and may result in the generation of supra-thermal electrons which subsequently preheat the laser target. In order to drive a symmetric target implosion, laser targets irradiated with short-wavelength laser light require a very high degree of radiation uniformity in the coronal plasma. Self-focusing results in nonuniform illumination of the target ablation surface, a possible enhancement of fluid instabilities, and a corresponding reduction in compression. It is therefore vital to study all of the factors which contribute to self-focusing of the incident laser light.

Filamentation has been studied intensively for the past several years, both analytically,¹⁻⁴ and by using numerical techniques.⁵⁻¹² Analytical work has given considerable insight into the behavior of filamentation. However, due to its highly nonlinear and often nonsteady-state nature, a much more detailed description is necessary, and this is possible using complex simulation codes. Here, we investigate self-focusing using a two-dimensional cylindrically symmetric Eulerian-plasma hydrodynamic code.¹³ As well as solving the plasma fluid and electron-ion temperature equations, the laser-light paraxial wave equation is solved numerically in order to account for diffraction and ponderomotive force terms. Because of their complexity, these effects are normally neglected in codes which use ray tracing, although they can be extremely important factors in self-focusing. The authors in Ref. 6 also used the paraxial wave equation to study laser light self-focusing. In their calculations, however, hydrodynamics was not included and a simple pressure balance was used to calculate perturbed densities due to the light wave. The importance of hydrodynamics to filamentation has already been realized,⁷ and, in particular, it is crucial for describing the off-axis

time-dependent focusing reported here.

Previous studies of filamentation in plasmas have concentrated on whole-beam focusing. Here, we are concerned with factors affecting the small-scale focusing which is induced by a nonuniformity superimposed upon a spatially uniform laser beam. This is a more realistic initial condition for self-focusing than would be a whole-beam Gaussian intensity distribution. The use of ray tracing in computer simulations has meant that thermal self-focusing has received much greater attention than ponderomotive self-focusing. Ponderomotive self-focusing can, in principle, self-focus the beam to higher intensities and much smaller scales than thermal self-focusing, since it is not limited by the electron conduction mean free path. The factor determining the scale of ponderomotive filaments is diffraction, and this is the main point addressed here. Recently, it was reported that laser light nonuniformities can drive small-scale ion fluctuations.¹⁰⁻¹² Simulations by Coggeshall, Mead, and Jones¹⁰ showed clearly the effect of ion fluctuations, namely, small-scale space- and time-dependent focusing of the laser flux. These authors used ray tracing in their code, and examined thermal self-focusing. In related studies, we have shown that ponderomotive forces can also effectively drive short-scale ion fluctuations.¹¹⁻¹² In this Letter, the sensitivity of time-dependent small-scale filamentation to diffraction is investigated.

The model for laser light propagation forms an important part of the present study, and so it is briefly described here. Specifically, we numerically solve the paraxial wave equation,⁹

$$\frac{\partial \zeta}{\partial z} = \frac{i\ell}{2k(z)} \nabla_{\perp}^2 \zeta - \frac{i}{2k(z)} Q \zeta, \quad (1)$$

where ∇_{\perp}^2 is the transverse Laplacian in cylindrical coordinates (perpendicular to the axial direction of propagation z), and

$$Q = \frac{\omega_p^2(r, z)}{c^2} \left(1 - \frac{n_e(0, z)}{n_e(r, z)} \right) - ik(z) K_{\text{abs}}(r, z) \quad (2)$$

accounts for refraction and attenuation. In Eqs. (1) and (2), ζ represents the laser-light complex flux amplitude (the intensity is $|\zeta|^2$), ω_p is the electron plasma frequency, n_e is the electron density, and K_{abs} is the absorption coefficient as a function of r and z . Taking $\iota=1$ in Eq. (1) specifies a diffraction-limited laser beam, while $\iota=0$ enables diffraction to be completely omitted.

We shall consider the propagation of a laser beam through an initially uniform hydrogen plasma with a density equal to 10% of the critical density (n_c) for laser light with $\lambda=0.25 \mu\text{m}$. The incident intensity at $z=0$ is fixed in time, and has a radial dependence defined by $I(r, z=0)=I_0(1+\epsilon e^{-r^2/\sigma^2})$, with $I_0=10^{15} \text{ W cm}^{-2}$. Inside the plasma ($z > 0$), the intensity has a z dependence due to inverse bremsstrahlung absorption. The function $I(r)$ is chosen as a simple model for hot spots in an imperfect laser field. In the diagrams, the laser propagates towards increasing z values and is symmetric around the z axis. The laser flux is plotted at grid points which coincide with the hydromesh, but is actually defined on its own more finely resolved mesh (the minimum mesh spacing is, however, restricted to the laser wavelength). This increases numerical accuracy, but any submicron hydrodynamic phenomena taking

place at large radii will not be modeled accurately since the radial mesh spacing on the hydrogrid is chosen to increase geometrically with r . In this Letter, however, the phenomena of interest originate near to the z axis, where there is adequate submicron mesh resolution ($\Delta r=0.25 \mu\text{m}$ at $r=0$).

Ponderomotive self-focusing has been investigated for a variety of hot-spot radii, σ , initial electron temperatures, T_e , and amplitudes, ϵ . Figure 1(a), in which $\sigma=100 \mu\text{m}$, $T_e=5 \text{ keV}$, $\epsilon=1$, and $\iota=1$ (the diffraction-limited case) is a typical example. The 5-keV initial temperature excludes thermal self-focusing and isolates ponderomotive force effects. It is clear that early in time, $t=35 \text{ ps}$, the laser light is breaking up into a number of filaments. This is caused by mainly radially propagating ion fluctuations; i.e., each small-scale filament is associated with a moving pit of density into which it is being focused. The density disturbances are initiated by the ponderomotive pressure of the nonuniform light wave, and it has been found that at later times the beam structure is insensitive to σ provided intensity thresholds are exceeded. Figure 1(b) shows the intensity later in time, $t=40 \text{ ps}$, and it can be seen that more structure is being added into the beam. To investigate diffraction, the previous calculation is repeated with $\iota=0$ (i.e., diffraction omitted). Figure 2(a) shows the corresponding laser intensity in the plasma at $t=12.5 \text{ ps}$, and

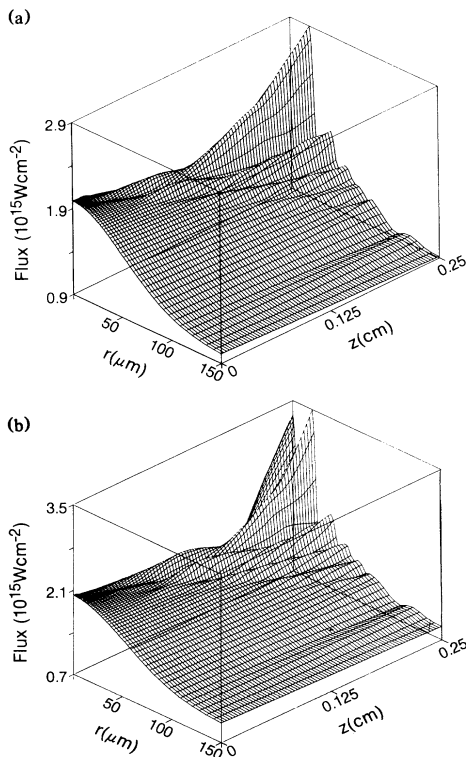


FIG. 1. Flux vs r and z for a Gaussian hot spot superimposed upon uniform-intensity plane laser light. Parameters used are (i) uniform intensity $=10^{15} \text{ W cm}^{-2}$, (ii) $T_e=T_i=5 \text{ keV}$, (iii) $n_e/n_c=0.1$, (iv) $\sigma=100 \mu\text{m}$, (v) $\epsilon=1.0$, (vi) $\iota=1.0$; (a) $t=35 \text{ ps}$, (b) $t=40 \text{ ps}$.

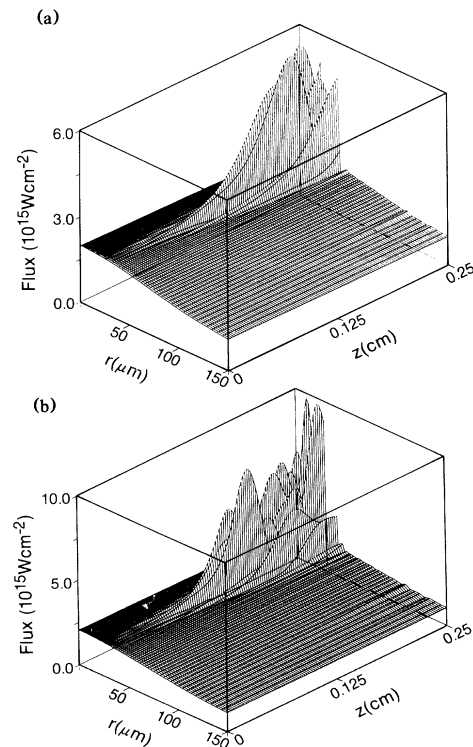


FIG. 2. Parameters as in Fig. 1, except $\iota=0$; (a) $t=12.5 \text{ ps}$, (b) $t=17.5 \text{ ps}$.

it can be seen that the beam again breaks up into a number of filaments. A comparison with Fig. 1 shows that in the absence of diffraction the scale size achieved is considerably less, and the intensity magnification is noticeably larger. Figure 2(b) shows the intensity at $t=17.5$ ps. Again, additional structure appears on the beam as time evolves. This is consistent with the generation of ion fluctuations by the ponderomotive forces associated with the filamented light. There are approximately ten intensity maxima across the radius of the hot spot in Fig. 2(b), as compared to five in Fig. 1(b). Self-focusing also starts earlier in time when diffraction is omitted, indicating that ponderomotive threshold intensities are sensitive to diffraction. Diffraction therefore has an appreciable effect on all aspects of the interaction.

Filamentation in the previous examples is taking place rapidly, in the sense that there is only a small difference between $t=0$ and the onset of the instability. In the following, we consider smaller amplitude hot-spot perturbations, and examine longer-scale plasmas. This will serve to demonstrate that small-scale focusing is possible for a wider range of plasma conditions. In Fig. 3, the laser flux corresponding to one such case is displayed at $t=1.32$ ns. The hot-spot amplitude corresponds to $\epsilon=0.5$, and diffraction is fully accounted for ($\iota=1$). The instability first turns on at $t\approx 1.1$ ns (much later than in previous examples), at which point the focusing length is approximately equal to the length of the simulation box. Just after the onset of the instability, density perturbations are observed which are localized towards $r=0$ at the maximum z position. It is then not possible for laser light refraction or diffraction (at smaller values of z) to spread the intensity to larger radii, as is the case in Fig. 1. Only later in time, as shown in Fig. 3, does the intensity structure spread radially outwards, due to the advection of density disturbances by the ponderomotively driven plasma flow. In this calculation, the density per-

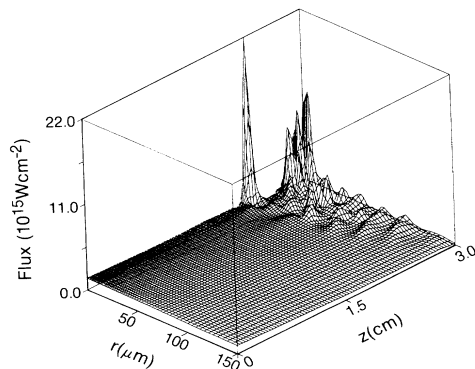


FIG. 3. Flux vs r and z for a Gaussian hot spot superimposed upon uniform intensity laser light. Parameters used are (i) uniform intensity $=10^{15}$ W cm $^{-2}$, (ii) $T_e=T_i=5$ keV, (iii) $n_e/n_c=0.1$, (iv) $\sigma=100$ μ m, (v) $\epsilon=0.5$, (vi) $\iota=1$; $t=1.32$ ns.

turbations have a radial scale size of between 5 and 10 μ m (corresponding to the approximate scale size of the intensity modulations), and they are located towards the end of the simulation region as above. During this particular simulation, the value of ϵ was increased slightly; $\epsilon=0.7$ was tried. This had the effect of shortening the focusing length and slightly increasing the amplitude of the intensity structures. Density fluctuations, moving out from near $r=0$, were then observed at smaller values of z . By increasing ϵ in the above manner, it is possible to drive small-scale focusing throughout the entire region simulated.

The previous calculation was also repeated with the diffraction term omitted, i.e., taking $\iota=0$. With $\epsilon=0.5$, self-focusing is observed much earlier in time; $t\approx 80$ ps as compared to $t\approx 1.1$ ns in Fig. 3. The focusing length is also approximately 10 times shorter, indicating that the neglect of diffraction has very serious consequences for this interaction. In an attempt to produce self-focusing at the end of the simulation box (as in Fig. 3), the value of ϵ was lowered. However, the main effect of this was to delay the onset of self-focusing. Figure 4 shows the laser flux just before very strong self-focusing (intensity magnification >100) occurs. In this figure $\epsilon=0.2$ is used, and the instability first occurs at $t\approx 120$ ps (compared to $t=80$ ps with $\epsilon=0.5$). The two intensity peaks, seen near $z=0$ in Fig. 4, grow rapidly within a subsequent time scale of 20 ps, and eventually multiple focusing occurs along the z axis. The laser flux again contains modulations in the $r-z$ plane, with scale sizes comparable to those shown in Fig. 2. Modulations occur at large radii early in time in this example, corresponding to laser light refraction by small-scale density perturbations located near to $z=0$. As in the above examples, the density perturbations spread out radially with time.

The effect of diffraction on thermal self-focusing was also investigated. In the simulations, this is achieved by artificially turning off the ponderomotive force and lowering the plasma temperature ($T_e=1$ keV, typically).

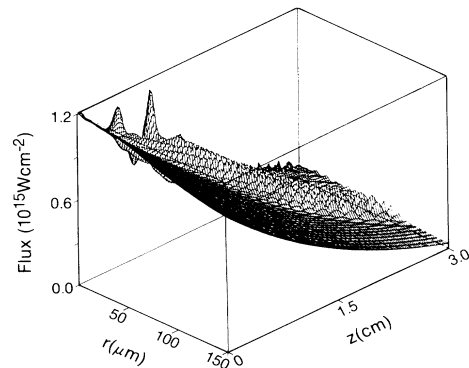


FIG. 4. Flux vs r and z for a Gaussian hot spot superimposed upon uniform intensity laser light. Parameters as in Fig. 3, except (i) $\iota=0$, (ii) $\epsilon=0.2$, (iii) $t=120$ ps.

In contrast to ponderomotive focusing (with diffraction accounted for), the thermal self-focusing length is short initially and is observed to lengthen (along z) only after the laser light has heated the plasma and caused it to expand. Typically, an intense focus occurs near $z=0$ which progresses towards the far end of the simulation box as time evolves. The thermal pressure associated with the focused light drives ion fluctuations which propagate radially outwards from the moving focus. Away from the z axis the light wave is again modulated due to the presence of the ion fluctuations. The scale size and amplitude of the off-axis intensity modulations are not significantly changed when diffraction is omitted. As mentioned previously, the scale sizes achieved with thermal self-focusing are generally larger than with ponderomotive self-focusing, and it is reasonable to expect that diffraction will have a greater effect on the latter than on the former, as is observed. The threshold intensity for thermal self-focusing to occur, in contrast to ponderomotive self-focusing, is relatively insensitive to diffraction. In one example, the threshold intensity increased slightly when diffraction was omitted. For the relatively small hot-spot radii considered, this is because the threshold intensity for thermal self-focusing decreases as σ increases. In the absence of diffraction the effective σ at any z position no longer increases with z , making it more difficult for focusing to occur. As expected, smaller radius hot spots demand larger intensities to initiate self-focusing, but once the focusing occurs it strongly resembles results obtained with larger radius nonuniformities.

In summary, we have investigated the effect of diffraction on laser light self-focusing in low-density plasmas, using a computational model which accounts for thermal transport, hydrodynamic motion, and laser beam propagation. Diffraction has an appreciable effect on ponderomotive intensity thresholds, and on scale sizes and focusing lengths achieved during filamentation. For example, in long-scale-length plasmas, the threshold intensity and focusing length (with $\sigma=100\ \mu\text{m}$) for ponderomotive filamentation decreases by an order of magnitude when diffraction is neglected. In contrast, the intensity threshold for thermal focusing is found to in-

crease slightly when diffraction is omitted (the smaller beam divergence makes it more difficult to form thermal gradients). Small-scale radially propagating ion fluctuations are observed when thermal or ponderomotive self-focusing occurs. The radial hydrodynamic flow of these fluctuations results in intensity modulations outside of the region of laser light nonuniformity. The results are insensitive to the transverse scale of the input nonuniformity provided that intensity thresholds for self-focusing are exceeded.

The authors extend thanks to Cray Canada for a substantial donation of computer time. This work was supported by the Natural Sciences and Engineering Research Council of Canada.

¹J. F. Drake, P. K. Kaw, Y. C. Lee, G. Schmidt, C. S. Liu, and M. N. Rosenbluth, *Phys. Fluids* **17**, 778 (1974).

²C. E. Max, *Phys. Fluids* **19**, 74 (1976).

³J. F. Lam, B. Lippman, and F. Tappert, *Phys. Fluids* **20**, 1176 (1977).

⁴R. Bingham and C. N. Lashmore-Davies, *Plasma Phys.* **21**, 433 (1979).

⁵A. B. Langdon and B. F. Lasinski, *Phys. Rev. Lett.* **34**, 934 (1975).

⁶S. Sartang, R. Evans, and W. T. Toner, *J. Phys. D* **16**, 955 (1983); D. J. Nicholas and S. G. Sajjadi, *J. Phys. D* **19**, 737 (1986).

⁷R. S. Craxton and R. L. McCrory, *J. Appl. Phys.* **56**, 108 (1984).

⁸K. Estabrook, W. L. Kruer, and D. S. Bailey, *Phys. Fluids* **28**, 19 (1985).

⁹R. Marchand, R. Rankin, C. E. Capjack, and A. Birnboim, *Phys. Fluids* **30**, 1521 (1987).

¹⁰S. V. Coggshall, W. C. Mead, and R. D. Jones, *Bull. Am. Phys. Soc.* **32**, 4T2 (1987); R. D. Jones *et al.*, *Phys. Fluids* **31**, 1249 (1988).

¹¹R. Rankin, R. Marchand, and C. E. Capjack, *Bull. Am. Phys. Soc.* **32**, 4T4 (1987).

¹²R. Rankin, R. Marchand, and C. E. Capjack, *Phys. Fluids* **31**, 2327 (1988).

¹³R. Rankin, A. Birnboim, R. Marchand, and C. E. Capjack, *Comput. Phys. Commun.* **41**, 21 (1986).